Available online at www.sciencedirect.com
SCIENCE DIRECT®
Journal of Power Sources 130 (2004) 1–7
JOURNAL OF POWER SOURCES
www.elsevier.com/locate/jpowsour

# Characterisation of the SOFC material, $LaCrO_3$, using vibrational spectroscopy

G.A. Tompsett [a], N.M. Sammes [b,*]

[a] *Department of Chemical Engineering, University of Massachusetts, Amherst, MA 01003, USA*
[b] *Connecticut Global Fuel Cell Center, University of Connecticut, 44 Weaver Road, CT 06269-5233, USA*

Received 5 September 2003; accepted 25 November 2003

**Abstract**

$LaCrO_3$ is reported to undergo a low to high temperature (HT) phase transition from orthorhombic (*Pnma*) to rhombohedral (*R*-3*c*), at ca. 255 °C. The phases involved in the low temperature phase transition of $LaCrO_3$ have been determined using Raman spectroscopy at temperatures from −196 to 300 °C. There are nine Raman bands observed from a total of 24 predicted modes, seven of which are assigned from comparison with the Raman profile and relative band positions observed and calculated for the isostructural compound, $YMnO_3$, as follows: 131($B_{2g}$), 150($B_{3g}$), 174($A_g$), 252($B_{1g}$), 279($A_g$), 441($A_g$) and 590($A_g$) $cm^{-1}$.

A phase transformation was observed at ca. 260 °C from the change in the Raman profile. The high temperature rhombohedral phase of $LaCrO_3$ had four bands which are assigned as follows: 58($E_g$), 161($E_g$), 288($A_{1g}$) and 434($E_g$, $E_g$) $cm^{-1}$, from comparison with the Raman profile and relative band positions observed for the isostructural compound, $NdAlO_3$.

The Fourier transform infrared (FTIR) spectrum of $LaCrO_3$ showed a total of eight bands discernible at room temperature from 25 predicted modes for the orthorhombic structure. The mode assignments were determined by comparison with the Raman profile and relative band positions observed and calculated for the isostructural compound, $SmAlO_3$, as follows: 138($B_{2u}$), 166($B_{3u}$), 197($B_{1u}$), 240($B_{3u}$), 266($B_{2u}$), 332($B_{2u}$), 357($B_{2u}$), 381($B_{3u}$), 425($B_{3u}$), 446($B_{1u}$), 471($B_{3u}$), 493($B_{3u}$), 573($B_{1u}$), 606($B_{3u}$) and 670 ($B_{1u}$) $cm^{-1}$.


*Keywords:* Lanthanum chromite; Raman spectroscopy; Infrared spectroscopy; Phase transition; Perovskite

## 1. Introduction

Doped $LaCrO_3$ is of interest as an interconnect material for solid oxide fuel cells, due to properties such as high electronic conductivity, stability in reducing environments, good thermal mismatch and good physical and chemical compatibility with other cell components. For example, Ca doped $LaCrO_3$ has an electrical conductivity at 1000 °C of 1–60 S/cm in an oxygen partial pressure range of $1.013 \times 10^{-5}$–$1.013 \times 10^{5}$ Pa [1]. $LaCrO_3$ is also of interest in the field of catalysis, where perovskites such as $LaCrO_3$ are among the most active for CO oxidation [2].

$LaCrO_3$ belongs to the perovskite class of structures and has been characterised using X-ray diffraction (XRD) [3]. The well established orthorhombic to rhombohedral phase transition of $LaCrO_3$ has been observed, using X-ray diffraction, to occur at ca. 255 °C [4]. This phase transition is succeeded by a transition to the ideal cubic structure at 1643 °C and the material melts at 2227 °C [5].

Little literature exists on the Raman spectrum of $LaCrO_3$, however, Raman spectra of rare earth chromites $GdCrO_3$ and $YCrO_3$ have been reported [6] and the band positions assigned to modes determined from single crystal spectra and lattice dynamic calculations of $YMnO_3$ and $LaMnO_3$ [7].

Raman spectroscopy has recently been used to investigate the isostructural perovskites $LaGaO_3$ and $LaFeO_3$ [8,9]. Bands observed in the spectra of these perovskite oxides were assigned to modes by comparison to the fully characterised spectrum of $SmAlO_3$ [10].

Several workers [11,12] have reported the infrared spectra of rare earth *ortho*-chromites, although these bands were not assigned. Band positions observed for $LaCrO_3$ are as follows: 325, 343, 372, 425, 580, 630, 640 and 675 $cm^{-1}$.

In this paper, Raman and infrared spectroscopy are used to investigate the phases of $LaCrO_3$ present at temperatures from −196 to 300 °C, to characterise the structure of the material at various temperatures. This was undertaken to

* Corresponding author. Tel.: +1-860-486-8379; fax: +1-860-486-8378.
*E-mail address:* sammes@engr.uconn.edu (N.M. Sammes).

0378-7753/$ – see front matter © 2004 Elsevier B.V. All rights reserved.
doi:10.1016/j.jpowsour.2003.11.057

gain vibrational data on this material compared to the known data reported from X-ray diffraction studies.

## 2. Experimental

$LaCrO_3$ was fabricated using a glycine nitrate pyrolysis technique as described by Chick et al. [13], followed by uniaxial pressing the powder at 30 MPa and isostatic pressing at 200 MPa into pellets of 15 mm diameter, using a Stanstead isostatic press. Samples were then sintered in alumina boats at 1600 °C for 10 h. A heating rate of 1 °C/min was used to 700 °C for binder "burnout" followed by a rate of 10 °C/min until 1600 °C. Thin (ca. 100 μm) discs were prepared for variable temperature Raman spectroscopy using #1000 and #4000 SiC polishing paper.

Powder X-ray diffraction was carried out initially to confirm the presence of a single phase. A Philips X'Pert system was employed, using Cu Kα radiation. A scanning rate of 0.02°/s was employed. The room temperature XRD pattern of $LaCrO_3$ showed the presence of a single orthorhombic phase matching JCPDS cards #33–0701 and #24–1016.

Raman spectroscopy was performed on samples of polished discs using a Jobin Yvon U 1000 double beam pass spectrometer equipped with a microscope stage for analysing small samples utilising 180° incident geometry. A spectra physics argon–ion laser was employed to excite laser Raman spectra using a 514.5 nm laser line at an incident power of ca. 7 mW. A water cooled Hammamatsu R943-02 photomultiplier tube was used for detection. Spectra were obtained using 500 μm slit width and the scanning rate used to collect the spectra was kept at 0.5 $cm^{-1}$ $s^{-1}$.

A LINKAM TMS-91 temperature stage attached to the microscope, linked to a thermal monitor, was used to heat the samples at pre-programmed rates to a maximum of 300 °C and minimum of −196 °C using liquid $N_2$. The spectra were obtained using an uncoated Olympus 50× objective lens over a range from 25 to 1000 $cm^{-1}$. A heating rate of 3°/min was used with 30 min equilibration time at each temperature.

Fourier transform infrared (FTIR) spectroscopy was carried out using a Digilab FTS-40 spectrometer couple with a PC computer. Mid-infrared spectra were obtained using direct transmission of KBr discs in the range 400–4000 $cm^{-1}$ averaging 64 scans at 8 $cm^{-1}$ resolution. Far-IR spectra where obtained using transmission of vaseline mulls on thin polyethylene plates. An evacuated bench was utilised and the spectral range of 50–500 $cm^{-1}$ with averaging of 256 scans at 8 $cm^{-1}$ resolution was employed. Spectral analysis was determined using GRAMS/32® software.

## 3. Results and discussion

As described in the introduction, $LaCrO_3$ can exist in three different solid phases: orthorhombic, rhombohedral and cubic, depending on the temperature. Raman and infrared spectroscopy can be used to determine the phase composition since the profile, the number of bands and the relative band positions are determined by the crystal symmetry of the compound. Using factor group analysis the number and type of vibrational modes, and hence bands predicted to be present in the spectrum, can be determined [14]. For the two lower temperature phases of $LaCrO_3$, factor group analysis has been performed to describe the number and type of modes predicted for the individual structures. Table 1 shows the irreducible representations for the cubic, orthorhombic and rhombohedral perovskite structures and those for the base oxides, $Cr_2O_3$ and $La_2O_3$, which have similar space groups. It can seen that the high temperature (HT) rhombohedral perovskite structure has a predicted total of five Raman active and eight infrared active modes compared to the lower symmetry orthorhombic structure, which has 24 Raman active and 25 infrared active modes.

The Raman spectrum of $LaCrO_3$ was obtained at various temperatures from −196 to 300 °C. The band positions are listed in Table 2. The $LaCrO_3$ sample displayed a black–green coloration and it is the likely cause of the poor signal-to-noise ratio observed in the spectra. However, there are six bands discernible at room temperature (20 °C) whereas an extra two bands are identified at liquid $N_2$ temperature (−196 °C). Fig. 1 shows a comparison of the Raman spectrum of $LaCrO_3$ at −196 and 20 °C (25–1000 $cm^{-1}$), and Fig. 2 shows a comparison of Raman spectra of $LaCrO_3$ at temperatures from −196 to 300 °C, in the range 25–600 $cm^{-1}$. With increasing temperature, the Raman profile does not differ significantly until 255 °C and

Table 1
Structures and irreducible representations for $La_2O_3$ and $Cr_2O_3$ base oxides and $ABO_3$ perovskites

| Structure $ABO_3$ | Space group | $Z$ | $\Gamma_R$ | $N_R$ | $\Gamma_{ir}$ | $N_{ir}$ | $N_i$ | $N_c$ | $\Gamma_{ac}$ |
|---|---|---|---|---|---|---|---|---|---|
| Rhombohedral A-$La_2O_3$ | *P*-3*m*1 $D^3_{3d}$ (164) | 1 | $2A_{1g} + 2E_g$ | 4 | $2A_{2u} + 2E_u$ | 4 | None | None | $A_{2u} + E_u$ |
| Rhombohedral α-$Cr_2O_3$ | *R*-3*c*, $D^6_{3d}$ (167) | 6 | $2A_{1g} + 5E_g$ | 7 | $2A_{2u} + 2E_u$ | 4 | None | None | $A_{2u} + E_u$ |
| Cubic (ideal) e.g. $SrTiO_3$ | P*m*3*m*, $O^1_h$ (221) | 1 | None | 0 | $3F_{1u}$ | 3 | $F_{2u}$ | 3 | $F_{1u}$ |
| Orthorhombic e.g. $GdFeO_3$ | *Pnma*, $D^{16}_{2h}$ (62) | 4 | $7A_g + 7B_{1g} + 5B_{2g} + 5B_{3g}$ | 24 | $7B_{1u} + 9B_{2u} + 9B_{3u}$ | 25 | $8A_u$ | None | $B_{1u} + B_{2u} + B_{3u}$ |
| Rhombohedral e.g. HT-$LaGaO_3$ | *R*-3*c*, $D^6_{3d}$ (167) | 6 | $A_g + 4E_g$ | 5 | $3A_{2u} + 5E_u$ | 8 | $3A_{2g} + 2A_{1u}$ | None | $A_{2u} + E_u$ |

*Key:* $\Gamma_R$, Raman modes; $\Gamma_{ir}$, infrared modes; $\Gamma_{ac}$, acoustic modes; R, Raman active; ir, infrared active; I, inactive; $N_R$, number of Raman active modes; $N_{ir}$, number of infrared active modes; $N_i$, number of inactive modes; *N*c: number of coincident modes; $Z$, number of formula units in the unit cell.

Table 2
Raman band positions ($cm^{-1}$) of $LaCrO_3$ at various temperatures

| −196 °C | 20 °C | 100 °C | 200 °C | 255 °C | 260 °C | 265 °C | 300 °C |
|---|---|---|---|---|---|---|---|
| 437 | 441 | | 434 | | 433 | 434 | 434 |
| 282 | 279 | | | | | | |
| 262 | 252 | | 258 | | | 252 | 258 |
| 180 | 174 | 176 | 168 | 162 | 162 | 162 | 159 |
| 153 | 150 | 149 | 148 | | | | |
| 131 | | | 140 | 141 | | | |
| 114 | 103 | | | 115 | 115 | | |
| 71 | | | | | 58 | 59 | 58 |

above, where none of the bands at 131, 153 and 282 $cm^{-1}$ (found at −196 °C) are observed. It should be noted that these three bands are not all found at 20–255 °C (Table 2), but all three completely disappear above 255 °C.

Several bands were also observed at high wavenumber positions (above ca. 600 $cm^{-1}$). The origin of these has not been determined, however they are possibly fluorescent/luminescent bands, as observed for other rare earth doped compounds [15]. Bands in the range 600–1200 $cm^{-1}$ have been reported for the Raman spectra of lanthanum–chromium oxide compounds [16]. Namely, $LaCrO_4$ has a sharp band at 830 $cm^{-1}$ and $La_2CrO_6$ has band at 865 $cm^{-1}$ [16]. Therefore, bands observed in the spectrum of $LaCrO_3$ at 600–1200 $cm^{-1}$ could be due to the presence of higher oxidation state chromium. Hydroxides and carbonates of lanthanum, for example, $La(OH)_3$, $La(OH)CrO_4$ and $La(CO_3)_3$ can occur as impurity phases in $LaCrO_3$ [16]. However, there is no evidence from the Raman spectra (Fig. 2) for these impurity phases. The band positions for these high wavenumber bands are listed in Table 3 for spectra obtained at −196, 20 and 300 °C. These bands appear to be relatively independent of those observed at wavenumber positions <600 $cm^{-1}$, although fewer are discernible due to the greater noise at higher temperature.

Table 3
High-wavenumber band positions observed for $LaCrO_3$ at various temperatures

| Temperature (°C) | Band positions ($cm^{-1}$) |
|---|---|
| −196 | 679 sh, 718 s, 735 sh, 746 sh, 763 sh, 794 w, 841 m, 920 w |
| 20 | 675 sh, 719 s, 790 m, 841 w, 918 w |
| 300 | 718 b, 842 s, 892 w, 916 w |

*Key:* w, weak; sh, shoulder; m, medium; s, strong; and b, broad relative intensity.

The band positions of the Raman spectrum of $LaCrO_3$ at −196 and 20 °C are compared to those observed for isostructural compounds $YMnO_3$, $YCrO_3$, $GdCrO_3$ and base oxides $Cr_2O_3$ and $La_2O_3$, as shown in Table 4. Assignment of the bands to vibrational modes is made on the basis of the comparison of the Raman profiles and the relative band positions to those of the fully characterised $YMnO_3$ compound. A

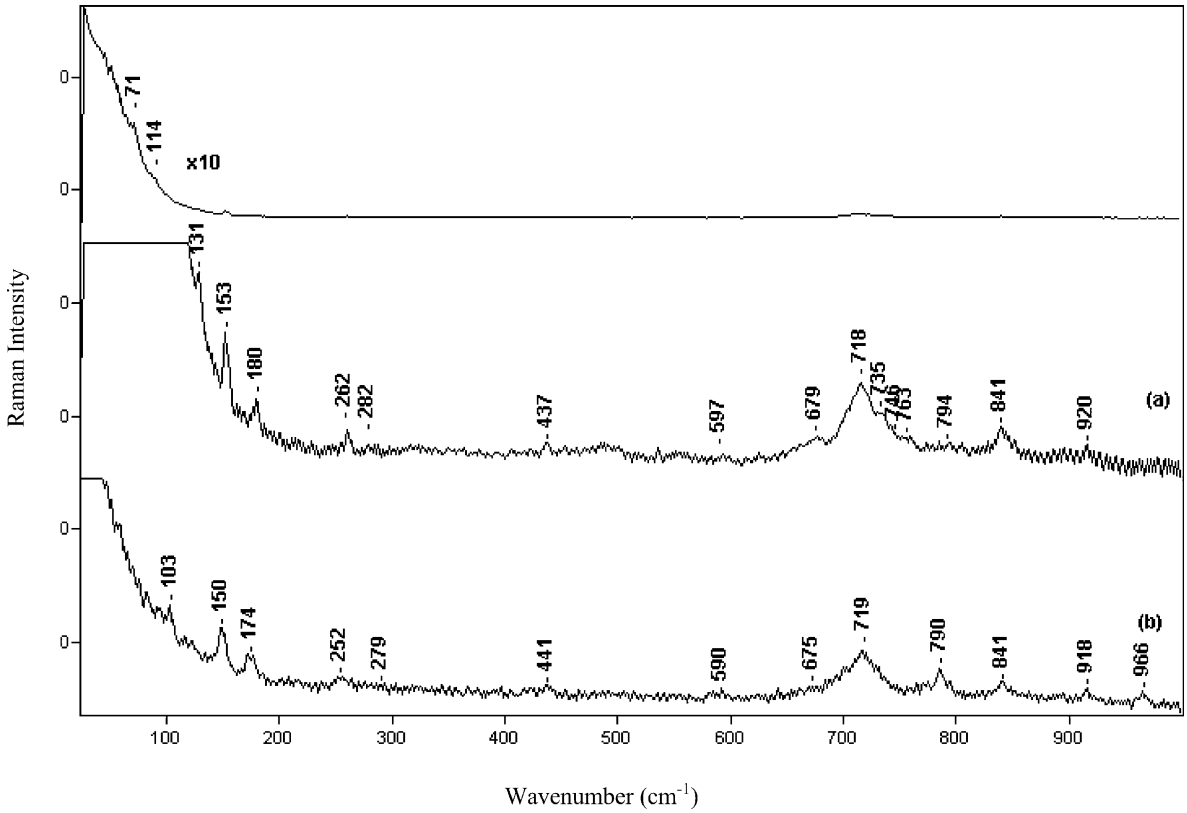


Fig. 1. Raman spectra of $LaCrO_3$ at (a) −196 °C and (b) 20 °C.

Table 4
Mode assignment of Raman band positions of orthorhombic $LaCrO_3$ phase

| Mode | $YMnO_3$ | | $YCrO_3$ [6,7] at RT | $GdCrO_3$ [6,7] at RT | $LaCrO_3$ band positions at | | $Cr_2O_3$ Band positions at RT [17] rhombohedral *R*-3*c* | $La_2O_3$ Band positions at RT [18] |
|---|---|---|---|---|---|---|---|---|
| | Exp. [7] | LDC [7] | | | 20 °C | −196 °C | | |
| | | | 700 | | 719 s | 718 s | 609($E_g$) | |
| | | | | | 675 sh | 679 sh | 551($A_{1g}$) | |
| $B_{2g}$ | 616 | 617 | | | | | | |
| $B_{3g}$ | | 610 | | | | | | |
| $B_{1g}$ | | 593 | | | | | | |
| $B_{2g}$ | 537 | 583 | | | | | | |
| $B_{3g}$ | | 476 | 569 | 568 | | | 530($E_g$) | |
| $A_g$ | 518 | 524 | 566 | 562 | 590 | 596 | | |
| | | | 514 | | | | | |
| $B_{2g}$ | 481 | 470 | 502 | 480 | | | | |
| $A_g$ | 497 | 466 | 492 | 480 | 441 | 437 | | |
| $B_{1g}$ | | 413 | | | | | | |
| $B_{3g}$ | | 390 | 487 | 472 | | | | |
| | | | | 394 $B_{3g}$ | | | | |
| $A_g$ | 396 | 407 | 429 | 390 | | | | |
| $B_{1g}$ | 383 | 342 | 413 | | | | | 410($E_g$, $A_{1g}$) |
| $A_g$ | 323 | 304 | 346 | 326 | | | | |
| $B_{2g}$ | 341 | 393 | 318 | 285 | | | ca. 397($E_g$) | |
| $B_{3g}$ | 336 | 363 | | | | | | |
| $B_{2g}$ | 317 | 285 | | | | | | |
| | | | | 282 $B_{2g}$ | | | 351($E_g$) | |
| $A_g$ | 288 | 223 | 282 | 260 | 279 | 282 | 303($A_{1g}$) | |
| $B_{1g}$ | 284 | 288 | 272 | 246 | 252 | 262 | | |
| $B_{1g}$ | 205 | 181 | | | | | | |
| | | | 240 | | | | | 195($A_{1g}$) |
| $B_{2g}$ | 220 | 162 | 223 | 161 | | | | |
| $A_g$ | 188 | 147 | 188 | 158 | 174 | 180 | | |
| $B_{3g}$ | 178 | 145 | 176 | 157 | 150 | 153 | | |
| $B_{2g}$ | 151 | 137 | 156 | | | 131 | | |
| $A_g$ | 151 | 104 | 156 | 141 | | | | 107($E_g$) |
| | | | 130 | | 103 | 114 | | |
| | | | 84 | | | 71 | | |

Observed at −196 °C; sh = shoulder, s = strong.

total of seven bands are assigned of the 24 predicted from factor group analysis. No bands due to the base oxides $Cr_2O_3$ and $La_2O_3$ are observed in the $LaCrO_3$ spectrum.

It can be seen from the decrease in the number of bands observed and the change in profile that there is a phase transition, which occurs above 260 °C (Table 2 and Fig. 2). Above 260 °C there are only four bands discernible, similar to the Raman profile observed after the orthorhombic to rhombohedral phase transition in $LaGaO_3$ [8].

The bands observed in the spectra obtained above 260 °C are assigned to the rhombohedral phase of $LaCrO_3$ as predicted from thermal data [3]. The band positions are compared to those reported for the fully characterised spectrum of the isosturctural compounds $NdAlO_3$ and high temperature-$LaGaO_3$ as shown in Table 5. Vibrational mode assignments to the observed bands are made on the basis of the Raman profiles and the relative band positions. Some similarities can be observed in the spectral profiles in the range 25–600 $cm^{-1}$. Further, the assigned Raman band positions of the base oxides $Cr_2O_3$ and $La_2O_3$, as described in Table 4, should be examined as they show the similarity between these and the perovskite material.

A further comparison is made between the isostructural orthorhombic compounds $LaCrO_3$, $YCrO_3$ and $GdCrO_3$ to evaluate the assignments of the relative band positions observed. This comparison was made by graphing the interatomic distances of $A^{3+}$–$O^{2-}$ and $B^{3+}$–$O^{2-}$ for the $ABO_3$ perovskite compounds versus the band positions observed for the $A_g$ stretching vibration above ca. 400 $cm^{-1}$ (shown in Fig. 3). Table 6 lists the average interatomic distances

Table 5
Mode assignment to band positions ($cm^{-1}$) of $LaCrO_3$ high temperature phase

| Mode | $NdAlO_3$ at RT [19] | HT-$LaGaO_3$ (500 °C) [8] | HT-$LaCrO_3$ (300 °C) [this work] |
|---|---|---|---|
| $E_g$ | 511 | 444 | 434 |
| $E_g$ | 511 | 444 | 434 |
| $A_{1g}$ | 243 | 232 | 258 |
| $E_g$ | 166 | 159 | 159 |
| $E_g$ | 55 | 55 | 58 |

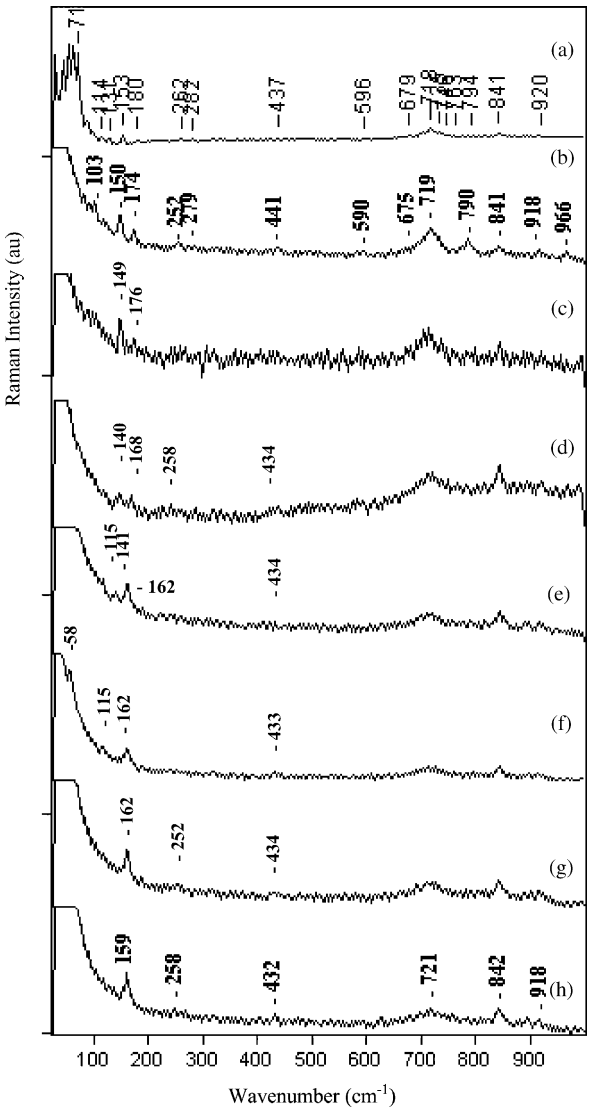


Fig. 2. Raman spectra of $LaCrO_3$ at (a) −196 °C; (b) 20 °C; (c) 100 °C; (d) 200 °C; (e) 255 °C; (f) 260 °C; (g) 265 °C and (h) 300 °C.

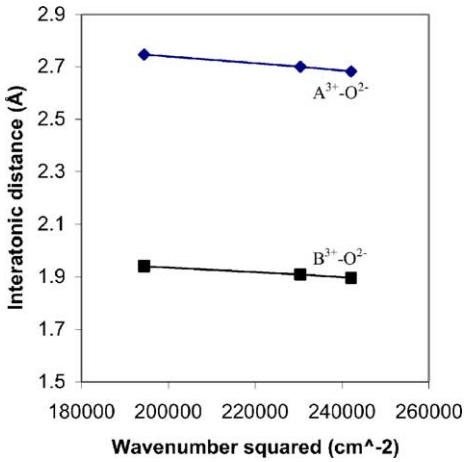


Fig. 3. Graph of interatomic distances of $A^{3+}$–$O^{2-}$ and $B^{3+}$–$O^{2-}$ vs. $A_g$ mode band positions for $ABO_3$ perovskites $YCrO_3$, $GdCrO_3$ and $LaCrO_3$.

and Raman band positions reported for compounds $LaCrO_3$, $YCrO_3$ and $GdCrO_3$.

In the perovskite structure, the A-site cation is surrounded by 12 oxygen ions whereas the B-site cation is bonded to six oxygen ions in the octahedral interstices of the oxygen sub-lattice [2]. Therefore, it is predicted that the vibrational modes associated with these atom motions should be sensitive to the force constants and hence bond distances. Fig. 3 shows that the graph of interatomic distances $A^{3+}$–$O^{2-}$ and $B^{3+}$–$O^{2-}$ for the $ABO_3$ perovskite versus the square of the band positions for the $A_g$ stretching vibration, which exhibits a linear relationship. This is consistent with Hooke's law where the bond length, and hence force constant, is proportional to the square of the vibrational frequency [14]. Therefore, this data supports the mode assignments made in Table 3 and that the bands observed above 600 $cm^{-1}$ are unlikely to be due to the normal modes of vibration for $LaCrO_3$. The relationship between band position and interatomic distance observed for the other assigned bands did not show as linear a dependence as this $A_g$ mode. The increase in A-site cation from $Y^{3+}$ to $Gd^{3+}$ to $La^{3+}$ affects both the $A^{3+}$–$O^{2-}$ and $B^{3+}$–$O^{2-}$ interatomic distances as observed in Table 3 and therefore the relationship between the bond lengths and band positions arising from the vibrations of the $BO_6$ octahedra may be more complex.

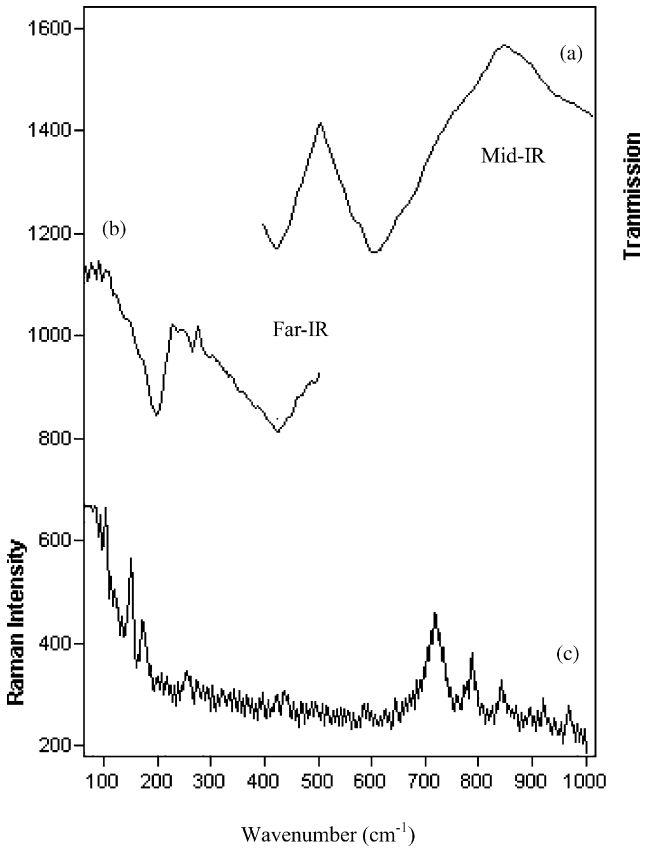


Fig. 4. Comparison of (a) mid-IR; (b) far-IR transmission spectrum and (c) Raman spectrum of $LaCrO_3$ at room temperature.

Table 6
Interatomic distances and Raman band positions for orthorhombic chromites

| Perovskite compound ($ABO_3$) | Average interatomic distance (Å) | | | Raman band positions ($A_g$ stretching mode) |
|---|---|---|---|---|
| | $A^{3+}$–$A^{3+}$ | $A^{3+}$–$O^{2-}$ | $B^{3+}$–$O^{2-}$ | |
| $YCrO_3$ [3] | 3.793 | 2.682 | 1.897 | 492 [7] |
| $GdCrO_3$ [3] | 3.820 | 2.701 | 1.910 | 480 [7] |
| $LaCrO_3$ [20] | 3.883 | 2.746 | 1.942 | 441 [this work] |

Table 7
Infrared band positions ($cm^{-1}$), relative intensities and vibrational assignment of $LaCrO_3$

| Mode | $SmAlO_3$ | | $LaCrO_3$ [this work] | $LaCrO_3$ [11] | Vibrational assignment [11] |
|---|---|---|---|---|---|
| | Observed [19] | Calculated [19] | | | |
| $B_{1u}$ | 670 | 668 | 670 sh | 675 sh | $\nu$Cr–O |
| $B_{2u}$ | 670 | 658 | | 640 s,b | |
| $B_{3u}$ | 670 | 678 | 606 s | 630 s,b | $\nu$Cr–O |
| $B_{1u}$ | ~650 | 651 | 573 sh | 580 s,b | |
| $B_{2u}$ | 580 | 583 | | | |
| $B_{2u}$ | 555 | 556 | | | |
| $B_{3u}$ | 525 | 521 | 493 sh | | |
| $B_{3u}$ | 525 | 515 | 471 sh | | |
| $B_{1u}$ | 495 | 504 | 446 sh | | |
| $B_{3u}$ | 460 | 432 | 425 s | 425 s,b | $\delta$O–Cr–O? |
| $B_{1u}$ | 430 | 424 | | | |
| $B_{1u}$ | 430 | 419 | | | |
| $B_{2u}$ | 430 | 412 | | | |
| $B_{3u}$ | N.O. | 405 | | | |
| $B_{3u}$ | 380 | 370 | 381 sh | 372 w,sp | $\delta$O–Cr–O? |
| $B_{2u}$ | 365 | 356 | 357 sh | 343 sh | $\delta$O–Cr–O? |
| $B_{2u}$ | 325 | 311 | 332 sh | 325 w,sp | |
| $B_{2u}$ | N.O. | 290 | 266 w | | |
| $B_{3u}$ | N.O. | 288 | 240 w | | |
| $B_{1u}$ | 220 | 212 | | | |
| $B_{1u}$ | 190 | 183 | 197 s | | |
| $B_{3u}$ | N.O. | 155 | 166 sh | | |
| $B_{2u}$ | N.O. | 144 | 138 sh | | |
| $B_{2u}$ | N.O. | 95 | | | |
| $B_{3u}$ | N.O. | 90 | | | |

*Key:* s, strong; w, weak; sp, sharp; sh, shoulder; and b, broad relative intensity; N.O., not observed.

Infrared spectroscopy was also used to characterise $LaCrO_3$, since much data has been reported on perovskite oxide materials [11,21,22]. Fig. 4 shows a comparison of the mid-IR and far-IR transmission spectrum and the Raman spectrum of $LaCrO_3$ at room temperature. It can be seen that their bands in the infrared spectrum are considerably broader than those in the Raman spectrum, however at least 15 features can be identified of the 25 predicted modes. The infrared band positions are listed in Table 7 and compared with fully characterised $SmAlO_3$ and band positions previously reported for $LaCrO_3$ [11]. Vibrational mode assignment to the observed band positions is made on the basis of the relative infrared spectral profiles and band positions of $SmAlO_3$ compared to $LaCrO_3$. It can be seen that the band positions observed for $LaCrO_3$ match closely with those reported by Subbu Rao et al. [11] although, several additional bands were identified, indicating that the composition is likely the orthorhombic perovskite structure as supported by the Raman data reported here. Thirteen bands were observed of the predicted and calculated 25 modes reported for the spectrum of $SmAlO_3$ [11]. Table 7 also lists the vibrational type assigned to the relative wavenumber ranges.

## 4. Conclusions

The phases involved in the low temperature phase transition of $LaCrO_3$ have been determined using Raman spectroscopy at temperatures from −196 to 300 °C. The 7 Raman bands observed from a total of 24 predicted modes were assigned from comparison with the Raman profile and relative band positions observed and calculated for the isostructural compound, $YMnO_3$, as: 131($B_{2g}$)[−196 °C], 150 ($B_{3g}$), 174($A_g$), 252($B_{1g}$), 279($A_g$), 441($A_g$) and 590($A_g$) $cm^{-1}$. Features at 71 and 103 $cm^{-1}$ are also observed.

A phase transformation was observed above 260 °C from the change in Raman profile observed. The high temperature rhombohedral phase of $LaCrO_3$ has four bands which are assigned from comparison with the Raman profile and relative band positions observed for the isostructural compound, $NdAlO_3$ as: 58($E_g$), 161($E_g$), 288($A_{1g}$) and 434($E_g$, $E_g$) $cm^{-1}$ (at 300 °C).

The FTIR spectrum of $LaCrO_3$ shows a total of 15 bands discernible at room temperature from 25 predicted modes for the orthorhombic structure. The mode assignments were determined by comparison with the Raman profile and relative band positions observed and calculated for the isostructural compound, $SmAlO_3$, as follows: 138($B_{2u}$), 166($B_{3u}$), 197($B_{1u}$), 240($B_{3u}$), 266($B_{2u}$), 332($B_{2u}$), 357($B_{2u}$), 381($B_{3u}$), 425($B_{3u}$), 446($B_{1u}$), 471($B_{3u}$), 493($B_{3u}$), 573($B_{1u}$), 606($B_{3u}$) and 670 ($B_{1u}$) $cm^{-1}$.

## Acknowledgements

G.T. would like to thank Dr John Seakins and the Chemistry Department, University of Auckland, New Zealand, for the use of the Raman spectrometer., This work was supported by the New Zealand Foundation of Research, Science & Technology, Contract UOW 402.

## References

[1] J.D. Carter, H.U. Anderson, M.G. Shumsky, J. Mater. Sci. 31 (1996) 551.
[2] B. Gilbu, H. Fjellvåg, A. Kjekshus, Acta Chim. Scand. 48 (1994) 37.
[3] S. Geller, Acta Cryst. 10 (1957) 243.
[4] S. Geller, P.M. Raccah, Phys. Rev. B4 (1970) 1167.
[5] J.-P. Coutes, J.M. Badie, R. Berjoun, J. Coutures, R. Flamand, A. Rouanet, High Temp. Sci. 13 (1980) 331.
[6] M. Udagawa, K. Kohn, N. Koshizuka, T. Tsushima, K. Tsushima, Solid State Commun. 16 (1975) 779.
[7] M.N. Iliev, M.V. Abrashev, H.-G. Lee, V.N. Popov, Y.Y. Sun, C. Thomsen, R.L. Meng, C.W. Chu, Phys. Rev. B 57 (1998) 2872.
[8] G.A. Tompsett, R. Phillips, N.M. Sammes, A.M. Cartner, Solid State Commun. 109 (9) (1998) 655.
[9] G.A. Tompsett, R.J. Phillips, N.M. Sammes, J. Aust. Ceram. Soc. 34 (1) (1998) 25.
[10] M.C. Saine, E. Husson, Spectrochim. Acta 40A (1984) 733.
[11] G.V. Subba Rao, C.N.R. Rao, J.R. Ferraro, Appl. Spectrosc. 24 (1970) 436.
[12] R.G. Darrie, W.P. Doyle, I. Kirkpatrik, J. Inorg. Nucl. Chem. 29 (1967) 979.
[13] L.A. Chick, L.R. Pederson, G.D. Maupin, J.L. Bates, J.G. Exharhos, Mater. Lett. 10 (1990) 1.
[14] G. Turrell, Infrared and Raman Spectra of Crystals, Academic Press, London, 1972.
[15] N. Kjerulf-Jensen, R.W. Berg, F.W. Poulsen, in: B. Thornstensen (Ed.), Proceedings for the Second European Solid Oxide Fuel Cell Conference, Ulf Bossell, Uberrohrdorf, Switzerland, 1996, p. 647.
[16] D.L. Hoang, A. Dittmar, M. Schneider, A. Turnschke, H. Lieske, K.-W. Brzezinka, K. Witke, Thermochim. Acta 400 (2003) 153.
[17] I.R. Beattie, T.R. Gilson, J. Chem. Soc. A 980 (1970).
[18] S.I. Boldish, W.B. White, Spectrochim. Acta 35A (1979) 1235.
[19] M.C. Saine, E. Husson, H. Brusset, Spectrochim. Acta 37A (1981) 985.
[20] S. Geller, V.B. Bala, Acta Cryst. 9 (1956) 1019.
[21] Y.Y. Kim, D.H. lee, T.Y. Kwon, H. Park, J. Solid State Chem. 112 (1994) 376.
[22] Y. Wu, Z. Yu, S. Liu, J. Solid State Chem. 112 (1994) 157.